Fractal geometry and the mapping of Efimov states to Bloch states

Ehoud Pazy*
Department of Physics, NRCN, P.O.B. 9001, Beer-Sheva 84190, Israel

(Received 1 May 2020; accepted 4 August 2020; published 25 August 2020)

Efimov states are known to have a discrete real-space scale invariance; working in momentum space we identify the relevant discrete scale invariance for the scattering amplitude defining its Weierstrass function as well. Through the use of the mathematical formalism for discrete scale invariance for the scattering amplitude we identify the scaling parameters from the pole structure of the corresponding zeta function; its zeroth-order pole is fixed by the Efimov physics. The corresponding geometrical fractal structure for Efimov physics in momentum space is identified as a ray across a logarithmic spiral. This geometrical structure also appears in the physics of atomic collapse in the relativistic regime connecting it to Efimov physics. Transforming to logarithmic variables in momentum space we map the three-body scattering amplitude into Bloch states and the ladder of energies of the Efimov states are simply obtained in terms of the Bohr-Sommerfeld quantization rule. Thus through the mapping the complex problem of three-body short-range interaction is transformed to that of a noninteracting single particle in a discrete lattice.

DOI: 10.1103/PhysRevE.102.022136

I. INTRODUCTION

The quantum physics of three-body resonantly interacting particles is known to generate a universal hierarchy of shallow three-body states as originally established by Efimov [1,2] for identical bosons. For a fairly recent review of the more general problem, e.g., treating the three-fermion state, the effect of dimensionality as well as an update on the experimental side, see [3]. For particles interacting through short-range attractive interactions that are nearly resonant the number of bound three-particle states, Efimov states, becomes infinite if at least two of the two-body interactions have an infinite s-wave scattering length. Aside from the amazing fact that these states are formed in a regime where two particles cannot bind, exhibiting what is referred to as Borromean binding, these three-particle bound states exhibit a discrete scaling symmetry. The discrete symmetry is manifested in the size R_n and binding energy E_n of the nth Efimov state, which scales spatially as $R_n = \lambda R_{n-1}$, and correspondingly for the energy as $E_n = \lambda^{-2} E_{n-1}$ with respect to the underlying $(n-1)$ Efimov state. For the homonuclear Efimov states the scale factor is given by $\lambda_0 = e^{\pi/s_0}$ where $s_0 = 1.006\,24$ is a universal constant.

Having eluded experimental verification for over three decades since their initial prediction, Efimov states were experimentally observed [4] and their universality has been demonstrated (see Ref. [5] for an experimental review). The experimental observation was facilitated by the ability to greatly enhance the scattering length in atomic systems via Feshbach resonances attaining low-energy universality in atomic few-body systems, which has led to a surge of theoretical and experimental effort in the study of few-body physics. Despite the large flow of experimental papers in which evidence of Efimov states was presented for homonuclear systems the experimental confirmation of the discrete scaling trait was long forthcoming. In 2014 two Efimov states of Cs atoms were subsequently observed [6] and three Efimov states were experimentally detected concurrently in heteronuclear Li-Cs mixtures at the University of Chicago [7] and in Heidelberg [8].

Originally of interest to the cold-atom and nuclear physics communities the importance of Efimov physics has been extended to many other fields. Only lately have aspects of Efimov physics been shown to be of relevance in solid state systems, particularly for topological semimetals and graphene. More specifically it has been shown to be related to quasi-Rydberg resonances in graphene and to physics of atomic collapse [9] as well as to interaction of an electron with an impurity in a Dirac semi-metal [10]. Recently the self-similarity of Efimov states was shown to extend to the time domain and ideas for observing the phenomena in cold-atom systems [11] and trapped ion systems have been suggested [12]. Amazingly also a connection between Efimov physics and the binding of three-stranded DNA, which is a classical system, was established [13–15], exhibiting in a sense what has been referred to as the biological Efmov effect.

On the theoretical side, Efimov first obtained his original solution employing hyperspherical coordinates [1,2]. Though originally met with skepticism the validity of Efimov's result was established both analytically and numerically by Amado and Noble [16,17]. Later the three-body system with short-range interactions was addressed in terms of an effective field theory (EFT) formulation of the problem [18–21]. Extensions of the theory beyond the three-body-system case have also been considered [22,23]. The scaling behavior of Efimov states is most evident when transforming the problem to an effective Schrödinger equation for a single particle in an inverse

*ehoudpazy@gmail.com

square potential [21]. The obtained Schrödinger equation is invariant under a continuous scale transformation, however, the problem is ill defined at short scales since the Hamiltonian is not self-adjoint. To remedy this issue one needs to impose a boundary condition, resulting in a remarkable result: the boundary condition breaks the continuous scale invariance spontaneously into a discrete scale symmetry. Such a breaking of a continuous scale symmetry in the quantum domain is a manifestation of a nonrelativistic scale anomaly [24]. Another notable issue is that the scaling factor is universal in the sense that it is independent of the chosen boundary conditions in terms of the renormalization group (RG); this effect is tied to the limit cycle behavior of the renormalization-group flow equation [25]. It was originally proposed by Wilson [26] that the RG equations can, in addition to fixed point solutions, also admit limit cycle solutions corresponding to a discrete scale invariance with respect to a scaling factor corresponding to the oscillation period. Such solutions exhibit a log-periodic dependence as a function of the characteristic scale. However, limit cycle RG solutions are quite rare and Efimov physics is probably the most notable example of such a solution [21,25].

Originally considered as an oddity in the energy spectrum of three particles with short-range interactions, Efimov physics has long been established to have profound connections to a wide range of physical problems. On the theoretical side the Efimov spectrum has been shown to form a geometric series corresponding to an infinite number of weakly bound states with an accumulation at the zero-energy threshold. The associated Efimov states thus posses a discrete scale invariance which is connected to a limit cycle RG limit. In this paper we focus on the geometrical aspect of Efimov states by employing the mathematical formalism for functions with discrete scale invariance (DSI); we identify the relevant scaling parameters and establish the appropriate Weierstrass function. The geometrical underlying fractal structure is identified, and finally, we use these observations to greatly simplify the problem by mapping it to that of a Bloch state.

The remainder of this paper is organized as follows. In Sec. II we give a brief introduction to Efimov physics, employing the EFT formulation. Specifically the scattering amplitude is calculated via EFT. The mathematics of functions possessing a DSI is shortly reviewed in Sec. III. The connection between scattering amplitude and DSI is established in Sec. IV based on a Neumann series expansion, and the corresponding Weierstrass function for the Efimov scattering amplitude is identified as well. In this section the underlying fractal structure of the scattering amplitude is established to be a ray across a spiral. Transforming to logarithmic variables Efimov states are mapped to Bloch states in Sec. V and the Efimov spectrum is obtained from the Bohr-Sommerfeld quantization rule. A brief discussion of the real-space formalism is presented in Sec. IV B. Results are discussed and summarized in Sec. VII.

II. EFIMOV PHYSICS IN TERMS OF EFT IN A NUTSHELL

It is convenient to introduce Efimov physics in terms of EFT; in this section we do so briefly for the sake of clarity. The presentation closely follows the method described in Refs. [19] and [21]. The basis for the EFT is the most general nonrelativistic Lagrangian for a boson field ψ with mass M, which is invariant under low-velocity Lorentz transformation and parity,

$$\mathcal{L} = \psi^\dagger\left(\imath\partial_0 + \frac{\nabla^2}{2M}\right)\psi - \frac{C_0}{2}(\psi^\dagger\psi)^2 - \frac{D_0}{6}(\psi^\dagger\psi)^3 + \ldots, \tag{1}$$

where C_0 and D_0 are the bare low-energy coupling constants for the two- and three-body interactions, respectively. To make the theory renormalizable it is defined up to an ultraviolet cutoff, Λ. Introducing a dummy field, d, corresponding to a local operator which annihilates two bosons at a point, the Lagrangian can be rewritten without the three- and the two-body contact interaction terms:

$$\mathcal{L} = \psi^\dagger\left(\imath\partial_0 + \frac{\nabla^2}{2M}\right)\psi + \Delta(d^\dagger d) - \frac{g}{\sqrt{2}}(d^\dagger\psi\psi + \text{H.c.}) + h(d^\dagger d\psi^\dagger\psi + \text{H.c.}). \tag{2}$$

Employing perturbation theory through a diagrammatic expansion in terms of Feynman diagrams, the first step involves calculating the dressed propagator for the dummy field, obtained by summing bubble diagrams to all orders. The next step is obtaining an integral for the Fourier transform of the amputated connected part of the Green's function $\langle 0|T(d\psi d^\dagger\psi^\dagger)|0\rangle$, resulting in a Skorniakov-Ter-Martirosian (STM) equation [27] for the scattering amplitude,

$$a_{\text{sc}}(p) = K(p,k) + \frac{2\lambda}{\pi}\int_0^\Lambda dq K(p,q)\frac{q^2}{q^2 - k^2 - i\epsilon}a_{\text{sc}}(q), \tag{3}$$

where $k(p)$ is the incoming (outgoing) momentum and $\lambda = 1$ for the bosonic case. For the case where a_2, the two-particle s-wave scattering length, satisfies the condition $1/a_2 \ll p \ll \Lambda$ and $k \sim 1/a_2$, the kernel in the integral, Eq. (3), is approximated by

$$K(p,q) = \frac{2}{\sqrt{3}q}\ln\left(\frac{q^2 + pq + p^2}{q^2 - pq + p^2}\right). \tag{4}$$

The main contribution to the integral comes from momenta in the intermediate region, $1/a_2 \ll q \ll \Lambda$, for which the following simplified integral equation can be obtained:

$$a_{\text{sc}}(p) = \frac{4}{\sqrt{3}\pi}\int_0^\infty \frac{dq}{q}a_{\text{sc}}(q)h(q,p), \tag{5}$$

where

$$h(q,p) = \ln\left(\frac{q^2 + pq + p^2}{q^2 - pq + p^2}\right). \tag{6}$$

The scale invariance of Eq. (6) suggests a power-law solution, $a_{\text{sc}}(p) \sim p^s$, to Eq. (5). Such a power-law solution requires that s satisfy the condition

$$1 - \frac{4}{\sqrt{3}\pi}\mathcal{M}_{h(q,p)}(s) = 0, \tag{7}$$

where $\mathcal{M}_{h(q,p)}$ is the Mellin transform with respect to the variable, q, and the transform is defined as

$$\mathcal{M}_{f(x)}(s) = \int_0^\infty dx\, x^{s-1}f(x). \tag{8}$$

There are two imaginary solutions to Eq. (7) given by

$$s = \pm \imath s_0 \tag{9}$$

with $s_0 \simeq 1.0064$. Thus the solution to Eq. (5) is given by the linear combination of

$$a_{\rm sc}(p) = c_+ p^{\imath s_0} + c_- p^{-\imath s_0}, \tag{10}$$

where $c_\pm$ are constants. In the above-mentioned region, $1/a_2 \ll p \ll \Lambda$, the phase of $a_{\rm sc}(p)$ is well determined,

$$a_{\rm sc}(p) = A \cos\left(s_0 \ln \frac{p}{\Lambda} + \delta\right), \tag{11}$$

where A and δ are some undetermined constants. It should be noted that the form of Eqs. (10) and (11) already suggests the underlying one-dimensional periodic physics on which we elaborate in Sec. V. In addition, the log periodic solution, (11), is a known property of functions with a DSI. In the following section we present, for the sake of clarity, a brief sketch of the properties of functions with DSI as a basis for establishing a connection to the three-body scattering amplitude.

III. A BRIEF INTRODUCTION TO DISCRETE SCALING FUNCTIONS

To help express the scattering amplitude in terms of functions with a DSI we briefly digress in this section to describe the mathematical properties of functions with a discrete symmetry. The material in this section is a short summary of the introductory material found in Ref. [28] combined with Ref. [29]. In general a function with a discrete scale invariance will obey the equation

$$f(x) = g(x) + \frac{1}{b} f(ax), \tag{12}$$

where a and b are scaling parameters and $g(x)$ is an initial function. In describing physical systems Eq. (12) typically becomes exact only asymptotically, however, for systems defined on regular geometrical fractals such as the Cantor set and the Sierpinsky gasket, etc., it is exact on all scales for nearest-neighbor interactions [30]. Thus functions satisfying Eq. (12) can usually be associated with a fractal structure.

The general solution to Eq. (12) is given by

$$f(x) = x^{\ln b/\ln a} G\left(\frac{\ln x}{\ln a}\right), \tag{13}$$

where $G(x)$ is a periodic function of x with period unity. A formal iterative solution of Eq. (12) is given in the form

$$f(x) = \sum_{n=0}^{\infty} b^{-n} g(a^n x). \tag{14}$$

In the specific case where $g(u) = \cos(u)$, where $u = a^n x$, one obtains the most well-known example of a continuous function which (for $ab > 1$) is nowhere differentiable introduced by Weierstrass [31] and named after him:

$$W(x) = \sum_{n=0}^{\infty} \left(\frac{1}{b}\right)^n \cos(a^n \pi x). \tag{15}$$

In the regime where the Weierstrass has a fractal structure one can associate with it a fractal dimension:

$$D_H = 2 + \frac{\ln b}{\ln a}. \tag{16}$$

For physical systems these sorts of solutions, Eqs. (14) and (15), are usually considered as an asymptotic case obtained for expansions close enough to a fixed point [30]. Performing a Mellin transform [defined in Eq. (8)], on Eq. (14) one obtains the zeta function for $f(x)$:

$$\zeta_f(s) = \frac{b a^s \zeta_g(s)}{1 - b a^s}. \tag{17}$$

The zeta function has the definition

$$\zeta_f(s) = \frac{M_f(s)}{\Gamma(s)}, \tag{18}$$

where Γ is the Euler gamma function.

The pole structure of $\zeta_f(s)$ in Eq. (17) is composed of poles of the analytical function g, which generally occur for integer values and contribute only to the regular part of f, and poles resulting from the DSI, which are given by the solutions s_n of

$$b a^s = 1. \tag{19}$$

Specifically

$$s_n = -\frac{\ln b}{\ln a} + \frac{2\pi \imath n}{\ln a}. \tag{20}$$

The $n = 0$ case gives the real power-law solution $f(x) = Cx^\alpha$ to the homogeneous version of Eq. (12), i.e., $g(x) = 0$, where $\alpha = -\frac{\ln b}{\ln a}$, which from Eq. (16) can also be presented as $\alpha = 2 - D_H$.

IV. DESCRIBING THE SCATTERING AMPLITUDE IN TERMS OF A DSI FUNCTION

Armed with the mathematics for DSI functions we can now return to the physics of the scattering amplitude, described in Sec. II, and attempt to reinterpret it in terms of self-similar structures. For convenience the corresponding equations for both the functions obeying a DSI and the scattering amplitude have been rewritten in Table I. In defining the connection it is of specific interest to find what the parameters a and b which define the scaling in Eq. (12) are for the case of Efimov physics. Furthermore, it is of interest to unmask the underlying fractal geometrical structure at the basis of the scattering amplitude.

A. Introducing a condition on the Neumann series solution to the EFT integral equation

In constructing a mapping between the integral equation for the scattering amplitude, (3), to Eq. (12), which defines functions possessing a DSI symmetry (see Table I; defining equation), we start by formally considering the iterative solution to the integral, Eq. (3), as a Neumann series as

$$a_{\rm sc}(p) = \sum_{n=0}^{\infty} \tilde{\lambda}^n \psi_n(p), \tag{21}$$

where $\tilde{\lambda} = 2\lambda/\pi$, $\psi_n(p) = \int_0^\Lambda dk \int_0^\Lambda \ldots \int_0^\Lambda \ldots K(p, q_1) K(q_1, q_2) \ldots K(q_n, k) dq_1 \ldots dq_n$, and $K(p, k)$ is defined by

TABLE I. Efimov and DSI corresponding equations.

Case	DSI	Efimov
Defining equation	$f(x) = g(x) + \frac{1}{b} f(ax)$	$a_{\rm sc}(p) = K(p,k) + \frac{2\lambda}{\pi}\int_0^\Lambda dq K(p,q)\frac{q^2}{q^2-k^2-i\epsilon}a_{sc}(q)$
Iterative solution	$f(x) = \sum_{n=0}^{\infty} b^{-n} g(a^n x)$	$a_{\rm sc}(p) = \sum_{n=0}^{\infty}\left(\frac{2\tilde{\lambda}}{\sqrt{3}}\right)^n \int_0^\Lambda dk K(a_e{}^n p, k)$
General solution	$f(x) = x^{\ln b/\ln a} G\left(\frac{\ln x}{\ln a}\right)$	$f_\pm(\tilde{x}) = e^{\pm \imath s_0 \tilde{x}} G\left(\frac{\tilde{x}}{\ln a_e}\right), \tilde{x} = \ln p$
Pole structure	$ba^s = 1$	$b_e \mathcal{M}_{h(q,k)}(s) = 1$
Poles	$s_n = -\frac{\ln b}{\ln a} + \frac{2\pi \imath n}{\ln a}$	$s_n^\pm = \pm \imath s_0 + \frac{2n\pi s_0}{\ln b_e}$

Eq. (4). Equation (21) can be rewritten in the form of the iterative solution, Eq. (14) (see Table I; iterative solution), for a DSI function under the condition

$$\int_0^\Lambda dq K(p,q)K(q,k) = \frac{2}{\sqrt{3}}K(a_e p, k), \tag{22}$$

where a_e is a parameter, currently unfixed, which can later be identified with the corresponding DSI parameter in Eq. (12) (see also Table I; defining equation). The equality in condition (22) is evident when applying a Mellin transformation to both sides [see Eq. (27)]. Essentially Eq. (22) is equivalent to the homogeneous form of Eq. (12) (see Table I; defining equation), in terms of the Green's function, since $\int dq K(p,q)K(q,k) = K(p,k)$, and employing this in Eq. (22) one obtains

$$K(p,k) = \frac{2}{\sqrt{3}}K(a_e p, k). \tag{23}$$

Thus by comparing Eq. (23) to the homogeneous form of Eq. (12) (see also Table I; defining equation), one obtains the scaling parameter $b \sim \sqrt{3}/2$ (up to the $\tilde{\lambda}^{-1} = \pi/2$ factor). Alternatively, under the condition in Eq. (22), Eq. (21) transforms to

$$a_{\rm sc}(p) = \sum_{n=0}^{\infty}\left(\frac{2\tilde{\lambda}}{\sqrt{3}}\right)^n \int_0^\Lambda dk K\left(a_e^n p, k\right). \tag{24}$$

From Eqs. (12) and (14) (see also Table I; defining equation and iterative solution), one can discern the scaling parameter $b_e = \sqrt{3}\pi/4$ and the periodic function

$$g_e(p) = \int_0^\Lambda dk K(p,k) \tag{25}$$

for the Efimov scattering amplitude. The index e was added to identify functions and parameters relevant to Efimov physics.

In Eq. (12) (see Table I; defining equation), the two DSI scaling parameters a and b were assumed to be fixed, defining the pole structure of the corresponding zeta function, Eq. (20) (Table I; poles). For the scattering amplitude for the Efimov physics these two parameters need to be inferred. Whereas the value of b_e is directly deduced from Eq. (24) (see Table I; iterative solution), the value of the parameter, a_e, needs to be established from the pole structure of the corresponding zeta function. Since the Efimov scattering amplitude obeys a DSI symmetry its parameters obey Eq. (19) (see Table I; pole structure), and since for Efimov physics $s = \pm s_0$ is fixed, a_e is automatically defined by b_e and s_0 as

$$a_e = \exp\left(\imath \ln b_e/s_0\right), \quad b_e = \frac{\sqrt{3}\pi}{4}. \tag{26}$$

To obtain this result in a more rigorous manner, one starts out by multiplying both sides of condition (22) by $p^{(s-1)}$ and integrating over p, thus obtaining

$$\frac{4}{3}\mathcal{M}_{h(p,q)}(s)\mathcal{M}_{h(q,k)}(s) = \frac{4}{3}a_e{}^{-s}\mathcal{M}_{h(p,k)}(s), \tag{27}$$

where the left-hand side of the equation is obtained from the Mellin convolution theorem. The condition for the Efimov scattering amplitude stated in Eq. (7), corresponding also to Table I (pole structure), can also be written as

$$\mathcal{M}_{h(q,k)}(s) = \frac{1}{b_e}. \tag{28}$$

Keeping in mind that $\mathcal{M}_{h(x,y)} \equiv \mathcal{M}_{h(x/y)}$, one obtains, upon inserting Eq. (28) (see also Table I; pole structure) into Eq. (27), exactly the condition for the pole structure of a DSI function defined in Eq. (19) (see Table I; pole structure). However, since this condition has to hold specifically for $s = \pm \imath s_0$ the value of a_e is thus fixed, but in contrast to the DSI functions discussed in the previous Sec. III, the parameter a_e for the scattering amplitude is complex. Furthermore, one should note that the parameter a_e is also a function of the scale parameter b_e, contrary to what is commonly the case, as they are usually fixed independently. These properties have consequences regarding the self-similar geometric structure which underlies the Efimov physics, as discussed shortly. As a side remark we note that the condition $b_e a_e^{\pm s_0} = 1$ for the Efimov states can be directly obtained from the self-similar nature of the scattering amplitude, $a_{\rm sc}(a_e p) = b_e a_{\rm sc}(p)$, by simply assuming a power-law solution $a_{\rm sc}(p) \sim p^{-s}$.

It is important to note that for the Efimov scattering amplitude, aside from the two poles $s^\pm = \pm \imath s_0$, the pole structure can take on the following values:

$$s_n^\pm = \pm \imath s_0 + \frac{2n\pi s_0}{\ln b_e}. \tag{29}$$

This pole structure should be contrasted with the DSI pole structure introduced in Eq. (20) (see Table I; poles), in which the real and imaginary terms are interchanged.

B. The corresponding Weierstrass function

Given the values of the DSI parameters, Eq. (26), and the function series for the scattering amplitude, Eq. (24) (see also

Table I; iterative solution), we can proceed and demonstrate that the scattering amplitude can be expressed as a Weierstrass function, Eq. (15). We begin by evaluating $g_e(p)$ defined in Eq. (25) by estimating the sum in Eq. (24) (see also Table I; iterative solution) by a saddle-point approximation. Taking the derivative in terms of n and defining $u = a_e{}^n x$ we obtain

$$(\ln b_e) g_e(u) + (\ln a_e) u g_e{}'(u) = 0. \tag{30}$$

Inserting the value of $a_e = \exp(\imath \ln b_e/s_0)$ from Eq. (26) into Eq. (30) simplifies the expression to

$$\frac{g_e'(u)}{g_e(u)} = \frac{\imath s_0}{u}, \tag{31}$$

from which $g_e(u)$ is obtained as

$$g_e(u) = \exp\left(\frac{\imath s_0}{u}\right). \tag{32}$$

However, a solution with the opposite sign is also admissible, Eq. (9), thus

$$g_e(u) = 2\cos\left(\frac{s_0}{u}\right). \tag{33}$$

Moreover, from the definition of $K(p,k)$ in Eq. (4) one obtains that $g_e(p) = g_e(\frac{1}{p})$ and so we obtain

$$g_e(u) = 2\cos\left(\frac{u}{s_0}\right). \tag{34}$$

By employing the above result, Eq. (34), and inserting the value of $g_e(p)$ into Eq. (24) (see also Table I; iterative solution), with the definition of b_e from Eq. (26), the Efimov scattering amplitude is expressed by a Weierstrass function, Eq. (15):

$$a_{\rm sc}(p) = 2\sum_{n=0}^{\infty} b_e^{-n} \cos\left(\frac{a_e^n p}{s_0}\right). \tag{35}$$

C. The underlying fractal structure

The DSI for the Efimov scattering amplitude is defined by the two scaling parameters, Eq. (26). Each iterative transformation multiplies the function by a constant factor $b_e = \sqrt{3}\pi/4$ and introduces a phase $a_e = \exp(\imath \ln b/s_0)$. It is natural to connect this symmetry to a one-dimensional scattering system, however, such a mapping does not convey the full underlying geometric fractallike structure at the basis of the DSI. To uncover the relevant underlying geometry, one should extend the one-dimensional form into the plane. Since the scale parameter a_e is complex it is convenient to consider the extension in terms of polar coordinates. We consider the scaling parameter b_e as a radius vector which is a function of the angle $b_e(\theta)$. As such this also introduces an angle dependence for $a_e(b(\theta))$. Since the periodicity requires $a_e(\theta + 2\pi) = a_e(\theta)$ one obtains the following constraint on b_e such that

$$\ln b_e(\theta + 2\pi) = \ln b_e(\theta) + 2\pi s_0. \tag{36}$$

To obey the above restriction, Eq. (36), b_e should be of a logarithmic spiral form,

$$b_e(\theta) = b_0 e^{\theta s_0}, \tag{37}$$

where now $b_0 = b_e$.

An alternative method to obtain the same result is obtained by considering Eq. (19) for $s^+ = \imath s_0$. In this case the condition can be written as

$$a_e{}^{\imath s_0} b_e = 1. \tag{38}$$

By the representation $a_e(\theta) = |a_e| \exp[\imath(\theta - \theta_0)]$ one obtains

$$b_e e^{\imath s_0 \ln(|a_e| e^{\imath(\theta-\theta_0)})} = b_e e^{\imath s_0 \theta \ln|a_e| - s_0(\theta-\theta_0)}. \tag{39}$$

Since $|a_e| = 1$, from Eq. (26) one again obtains Eq. (37) by identifying $b_0 = \exp(-s_0\theta_0)$.

In general the logarithmic spiral in terms of polar coordinates (r,θ) is defined by two parameters, c and α, such that $r = c\exp(\alpha\theta)$. It possesses the following interesting property, which is highly relevant to the DSI as well as the Efimov physics: the logarithmic spiral is a self-similar structure in the sense that scaling by a factor $\exp(2\pi\alpha)$ results in the same structure, and as a result, any ray from each center meets the spiral at distances which are a geometric progression. Thus one can infer from Eq. (37) that in the case corresponding to Efimov physics the spiral parameter α can be identified as $\alpha = s_0$. Thus the fractal nature of the Efimov scattering amplitude is identified as a logarithmic spiral which is obtained by rotating by 2π and stretching, where the scaling parameter, a_e, is responsible for the rotation, and the scaling parameter, b_e, for the stretching or shrinking of the function. The related geometric procedure can be viewed in the following way. Moving along the spiral an angle of 2π and rescaling the radius by b_e, one returns to the initial position.

D. Obtaining the expression for the scattering amplitude from the DSI formulation

Based on the knowledge gained regarding functions with DSI (see Sec. III) the expression for the Efimov scattering amplitude, Eq. (11), previously obtained by solving the relevant integral STM, Eq. (3) (see also Table I; defining equation), can now be realized directly by the mapping. Starting with the general solution of Eq. (12) (see Table I; defining equation) given in Eq. (13) (see Table I; general solution) in which $G(y)$ is an arbitrary periodic function of its argument y with period 1, considering the scaling parameter a_e as given by Eq. (26) with two possible complex values for $s^{\pm} = \pm\imath s_0$, and expressing the solution in terms of a logarithmic variable $\tilde{x} = \ln p$,

$$f_{\pm}(\tilde{x}) = e^{\pm\imath s_0 \tilde{x}} G\left(\frac{\tilde{x}}{\ln a_e}\right). \tag{40}$$

The above solution, Eq. (40), involves the two scales of the three-body physics; the short-length-scale physics is defined by the periodic function $G(y)$ and the long-length-scale physics is described by the plane wave. Taking the limit in which one can replace the periodic function $G(y)$ with a constant, the long-scale solution is given by the solution obtained by a linear combination of the $e^{\imath s_0 \tilde{x}}$ and $e^{-\imath s_0 \tilde{x}}$. Reexpressing the result in terms of p again, one obtains the known result [19] for the scattering amplitude $f_{\rm sc}(p) = A\cos[s_0 \ln(p/\Lambda) + \delta]$, where δ is some phase to be determined by the boundary conditions. We proceed below to demonstrate that under this different viewpoint a reinterpretation of the three-body physics can be given in terms of Bloch functions on a

TABLE II. Efimov, DSI, and Bloch correspondence.

State	DSI	Efimov	Bloch
Coordinate	x	$\tilde{x} = \ln p$	x
Poles	$s_n = -\frac{\ln b}{\ln a} + \frac{2\pi\imath n}{\ln a}$	$s_n^{\pm} = \pm\imath s_0 + \frac{2n\pi s_0}{\ln b_e}$	$k = \frac{2\pi n}{L}$
Relevant function	Weierstrass function	Scattering amplitude	Bloch wave function
Symmetry	$W(x) = \sum_{n=0}^{\infty} \left(\frac{1}{b}\right)^n \cos(a^n \pi x)$	$a_{\rm sc}(\tilde{x}) = e^{\imath k\tilde{x}} G\left[\frac{\tilde{x}}{L}\right]$	$\psi(x) = e^{\imath kx} u(x)$
	Scale invariance	Scale invariance (p), translation invariance ($\tilde{x}$)	Translation invariance
Geometrical structure	Fractal	Spiral	1D lattice
Relevant transform	Mellin	Mellin	Fourier series

one-dimensional lattice. In this reformulation the root of the zeta function, s_0, is analogous to the wave number and $\tilde{x} = \ln p$ is analogous to the spatial dimension along the one-dimensional lattice.

V. MAPPING EFIMOV STATES TO BLOCH STATES ON A ONE-DIMENSIONAL LATTICE

In this section we use the DSI formalism to map the three-body Efimov physics into that of a single particle confined to a one-dimensional discrete lattice.

A. Identifying the crystal momentum and lattice constant

Equation (24) (see Table I; iterative solution), for the three-body Efimov scattering amplitude, in terms of outgoing momenta p, was identified with the iterative solution, Eq. (14) (see Table I; iterative solution), of the STM, Eq. (3) (see Table I; defining equation). Through the similarity between the two equations the two scaling parameters, a_e and b_e, were identified [see Eq. (26)]. Based on this mapping the Efimov scattering amplitude can be expressed in terms of the general solution for functions obeying a DSI, Eq. (13) (see Table I; general solution), using the scaling parameters and transforming to a logarithmic variable, $\tilde{x} = \ln p$,

$$a_{\rm sc}(\tilde{x}) = e^{\imath k\tilde{x}} G\left[\frac{\tilde{x}}{L}\right], \tag{41}$$

where we have defined $k \equiv \imath(\ln b_e/\ln a_e)$, $L = -\imath \ln a_e$, and $G(x)$ is a periodic function with period 1. The similarities between the Efimov scattering amplitude, functions with a DSI, and Bloch functions are reported in Table II and graphically represented in Fig. 1. To better understand the correspondence between the Efimov scattering amplitude and the physics of a particle on a one-dimensional lattice we consider the pole structure of a function obeying a DSI as defined in Eq. (20) (see Table I; poles) and its analog in terms of Efimov physics, Eq. (29) (see also Table I; poles), expressing these in terms of k and L,

$$s = \imath k + \frac{2\pi n}{L}, \tag{42}$$

where the following identifications were considered:

$$s_0 \leftrightarrow k,$$
$$s_0/\ln b_e = -\imath/\ln a_e \leftrightarrow 1/L. \tag{43}$$

In this form the connection of $2\pi n s_0/\ln b_e$ to a crystal momentum is self-evident. It should be noted that whereas the pole structure for the DSI functions as well as for the Efimov scattering amplitude was obtained via a Mellin transform, the quasimomentum for the Bloch states is obtained by a Fourier series expansion. However, the two transforms can be connected if one considers the analytical continuation for the Mellin transform for a logarithmic variable.

The connection between the relevant underlying symmetries, the DSI invariance of the Efimov physics to the translation symmetry of the one-dimensional lattice system becomes clear by considering Eq. (43). One should note that considering a logarithmic variable $\tilde{x} = \ln p$ multiplication of the momentum p in the Efimov scattering amplitude by a constant a_e translates in terms of the logarithm variable, $\tilde{x}$, to a shift of $\tilde{x}$ in Eq. (41) by $\ln a_e$. This shift results only in a phase $\exp(\imath kL)$ since the function $G(x)$ in Eq. (41) is a periodic function with period 1. The phase, according to the identifications in Eq. (43), is $s_0 L = \ln b_e$. Making it clear that requiring that the Efimov scattering amplitude as described in Eq. (41) be viewed as the Bloch function on a lattice with a lattice period $L = \ln b_e/s_0$ defined by the condition $\psi(x + L) = \exp(\imath kL)\psi(x)$ is equivalent to requiring DSI symmetry. Thus identifying the scattering amplitude, Eq. (41), with a Bloch

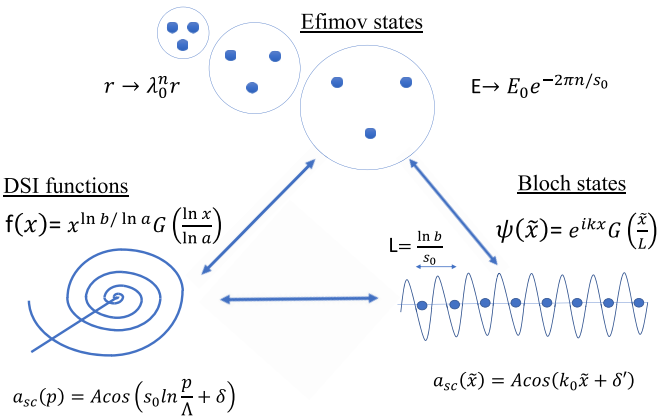

FIG. 1. Starting with the wave function for the Efimov states in real space transforming to momentum space and considering the scattering amplitude, the logarithmic spiral self-similar geometry is obtained. Transforming to exponential coordinates maps the physics into the physics of Bloch states on a one-dimensional lattice.

function through the definitions in Eq. (43) leads directly to the connection between the two underlying symmetries, i.e., multiplying p by a_e is equivalent to dividing or multiplying the function by b_e, which exactly defines the DSI.

Having established the analogy to Bloch states one can now view the Efimov physics in terms of the logarithmic variable $\tilde{x}$ as describing the physics of a particle on a one-dimensional lattice, where $\ln a_e$ plays the role of the lattice constant L and s_0 plays the role of the particle's momentum. The power-law ansatz $a_{sc}(p) \sim p^s$ suggested as a solution to Eq. (5) [19] simply maps into a plane-wave solution $a_{sc}(\tilde{x}) \sim \exp(\imath \tilde{x} s_0)$, where s is limited to the values $\pm \imath s_0$.

To make this analogy more explicit we consider the scattering amplitude, Eq. (11), expressed in terms of the logarithmic variable $\tilde{x} = \ln p$; we can now reinterpret it in terms of a Bloch state,

$$a_{sc}(p) = A \cos\left(s_0 \ln \frac{p}{\Lambda} + \delta\right) \rightarrow a_{sc}(\tilde{x}) = A \cos(k\tilde{x} + \delta'), \tag{44}$$

where δ' is a phase. In this representation the incoming momentum (in the Efimov description) plays the role of the spatial coordinate and s_0 plays the role of an effective crystal momentum.

B. Obtaining the Efimov spectrum from the Bohr-Sommerfeld quantization

Employing the connection between Efimov physics and Bloch functions and having identified the corresponding momentum through Eq. (43), the Efimov spectrum can now simply be obtained from the Bohr-Sommerfeld quantization rule,

$$s_0 \int_{\tilde{x}_1}^{\tilde{x}} d\tilde{x} = (n + \delta)\pi, \tag{45}$$

where δ is a phase resulting from the boundary conditions. Keeping in mind that the spatial coordinate is actually the logarithm of the momentum in the Efimov description $\tilde{x} = \ln p$, expressing Eq. (45) in terms of p, performing the integration, and employing the viral theorem, we obtain the Efimov spectrum

$$E_n = -\frac{p_*^2}{m} e^{-2\pi n/s_0}, \tag{46}$$

where $p_* = e^{-\delta\pi/s_0} \ln \tilde{x}_1$.

VI. REAL-SPACE FORMALISM

In this section we analyze Efimov physics in real space, thus we are able to connect it with the physics of the relativistic atomic collapse, which is defined through the same fractal geometry, that of a ray across a logarithmic spiral.

A. The Efimov connection to DSI in real space

In considering an operator with a Weierstrass spectrum γ^n, where n is an integer, it was shown [32] that the Schrödinger equation for the inverse square potential of the form

$$U(x) = -\frac{A}{x^2} \tag{47}$$

has an infinitely deep spectrum with states clustering at $E = 0$,

$$E_n = -E_0 \gamma^n, \tag{48}$$

referred to as a Weierstrass spectrum. When one requires that two solutions with energies E_1 and E_2 are orthogonal the ratio between these energies is given by

$$\frac{E_1}{E_2} = \exp\left(\frac{2\pi n}{\sqrt{A - \frac{1}{4}}}\right), \tag{49}$$

where n is an integer. To obtain the Weierstrass spectrum, Eq. (48), the constant A, in Eq. (47), defining the potential takes the value

$$A = \frac{1}{4} + \frac{4\pi^2}{\ln^2 \gamma}. \tag{50}$$

The above result relates directly to Efimov physics since in the real-space calculations using hyper-spherical coordinates for the three-body problem Efimov physics emerges from a Schrödinger equation with an inverse squared potential [21]. Given for convenience in coordinates in which $\hbar = 1$,

$$-\frac{1}{2\mu}\left[\left(\frac{d^2}{dR^2}\right) + \frac{{s_0}^2 + 1/4}{R^2}\right]\psi(R) = E\psi(R), \tag{51}$$

where $R \equiv= \frac{2}{3}(r_{12}^2 + r_{13}^2 + r_{23}^2)$, and r_{ij} are the relative particle coordinates, μ is the effective mass, and E is the energy of the bound state. Comparing Eqs. (47) and (50) to Eq. (51) one obtains the following identification:

$$s_0 \leftrightarrow \pm \frac{2\pi}{\ln \gamma}. \tag{52}$$

Considering a semiclassical-type solution using units in which the mass of the particles is $m = 1$ [33], the action given by

$$S = \pm \imath \int^{R_0} dR' k(R'), \tag{53}$$

where $k(R) = \sqrt{[E - V(R)]}$, and $V(R) = (s_0^2 + 1/4)/R^2$, which can be identified with $U(x)$ in Eq. (47) by employing the connection in Eq. (52) and applying it to Eq. (50). In the region of small R where E can be neglected the boundary conditions for the integral are given by the turning point R_0, which are the roots of $s_0^2 + 1/4 = 0$,

$$\psi(R) \approx A_+ e^{\left(\frac{1}{2} + \imath s_0\right)\ln R} + A_- e^{\left(\frac{1}{2} - \imath s_0\right)\ln R}, \tag{54}$$

where A_+ and A_- are constants.

According to the semiclassical Bohr-Sommerfeld approximation the phase difference between the two cases should be quantized such that

$$2s_0 \ln(R) = 2\pi n. \tag{55}$$

The Bohr-Sommerfeld condition, Eq. (55), thus defines the discrete periodicity of $k(R) \sim \ln R$ which is at the heart of Efimov physics and DSI functions. Equation (55) is equivalent to Eq. (45) and hence also leads to the spectrum in Eq. (46).

Similar physics is described in Ref. [34] in which the problem of atomic collapse in the relativistic regime is analyzed. It is worth mentioning since in this case the spiral geometry is clearly evident. The collapsing trajectories for an electron into the nucleus are best defined through the quasiclassical radial momentum equation,

$$p_R^2 = v_F^{-2}\left(E + \frac{Ze^2}{R}\right)^2 - \frac{M^2}{R^2}, \tag{56}$$

where R is the radial distance to the nucleus, p_R is the radial momentum, e the electron charge, Z the atomic number, M the electron angular momentum, and v_F the Fermi velocity. The spiral trajectories are directly manifest in the atom collapse by the collapse criterion defined in terms of the classical relativistic dynamics where the collapse occurs for the case where $M < Ze^2/c$ for $E > 0$. In this case the ray across the spiral is manifested from quantum mechanics considerations by the tunneling case in which $M < Ze^2/c$ for $E < 0$. It is currently impossible to actually experimentally observe atomic collapse in nuclei since the condition for it to occur is $Z > 170$. However, in Ref. [34] it has been suggested that the phenomena might be observed in graphene due to its large "fine-structure constant" $\alpha = e^2/\hbar v_F$. In this case the resulting spectrum for the problem is equally spaced on a log scale,

$$E_n \approx \frac{Ze^2}{r_0} e^{-\pi\hbar n/\gamma}, \tag{57}$$

where r_0 is a lattice cutoff, $\gamma = (M_c^2 - M^2)^{\frac{1}{2}}$, and $M_c = Ze^2/v_F$ is the critical angular momentum separating the falling trajectories from the stable trajectories.

Though Efimov physics, which is inherently three body, seems at first glance to be completely unrelated to the relativistic atomic collapse, upon deeper inspection similarities between the two systems can be observed. Both systems exhibit a collapse, the Thomas collapse in the case of Efimov physics [3], compared to the atomic collapse. With regard to graphene the massless Dirac particles cannot form bound states, similar to the Efimov condition that two particles cannot bind. The infinite number of bound Efimov states and the infinite number of quasibound states in the atomic collapse system both can be obtained from semiclassical considerations. Finally, there is the underlying fingerprint of the logarithmic spiral, the fractal structure at the heart of both phenomena.

It should also be noted that the Efimov physics is a special case in a more general set of problems which involve a singular inverse square potential. This set of equations also has a very similar dependence on a critical scale as the relativistic atomic collapse case, such that in order to obtain a discrete energy spectrum it is needed that in the potential, Eq. (47), $A > A_{\rm cr}$, where $A_{\rm cr} = (d-2)^2/4$ and d is the dimension of the problem. Stated this way the discrete spectrum is given by

$$E_n \propto e^{\frac{2\pi n}{\Lambda}}, \tag{58}$$

where $\Lambda = \sqrt{A - A_c}$ and the results are presented in units such that $\hbar = 1$.

VII. DISCUSSION AND SUMMARY

Efimov physics has been shown to be of importance to a wide set of physical problems ranging from ultracold atomic gases [4] through nuclear physics [35] to recently condensed matter systems [36] as well as to biological systems [13]. On the theoretical side it has even been considered for more than three particles for which it was originally formulated [22,23]. In this work we have examined the less studied aspects of the geometric and more specifically the fractal properties of the Efimov scattering amplitude. Whereas initially it was known that the Efimov spectrum forms a geometric series corresponding to an infinite number of weakly bound states which possess a discrete scale invariance, later also connected to a limit cycle RG limit, here we have demonstrated how one can apply the mathematical formalism for functions with DSI to the Efimov scattering amplitude. There are, however, some differences; in contrast to the theory described for functions possessing DSI symmetry in which one considers the two scaling parameters a and b as independent and fixed from the geometry determining the value of s_0, the zeroth pole of the corresponding zeta function, in the case of Efimov physics s_0 is imaginary and is obtained as a solution to a transcendental equation and b_e is fixed and real. Solutions can then be found by considering complex values for a_e. Using the DSI mathematical formalism we identified the relevant scaling parameters and established the corresponding Weierstrass function.

A fractal is an iterative structure. Famous examples are the triadic Cantor set obtained iteratively by dividing a segment into three parts, removing the middle part, and continuing the process with the remaining segments. Another example is the Sierpinski gasket, in which an equilateral triangle is subdivided recursively into smaller equilateral triangles. With regard to the Efimov scattering amplitude we have shown that the relevant fractal structure is a logarithmic spiral which is obtained by rotating by 2π and stretching, thus leaving the shape invariant. From the physics standpoint Efimov physics is an example of a scale anomaly where the classical system possesses a continuous symmetry which is broken at the quantum level to a discrete symmetry. In terms of our reformulation of the problem a new connection between the physical symmetry of the system and the underlying geometrical fractal can be established. The underlying continuous structure corresponding to Efimov physics is apparent from the fact that a_e is a complex number, thus multiplying by a_e induces a rotation followed by a stretching/contraction through multiplying the function by b_e. The one-dimensional mapping presented in the Sec. V results by considering the discrete values along a ray through a logarithmic spiral such that the angular coordinate θ of the spiral is restricted to a fixed angle. The self-similarity of the scattering amplitude for Efimov physics expressed geometrically through the logarithmic spiral turns into translation invariance up to a phase when transforming into a logarithmic variable allowing the mapping of the complex Efimov physics to that of a particle on a one-dimensional lattice. The mapping allowed us to obtain the Efimov spectrum from the Bohr-Sommerfeld quantization rule. Returning to the field theoretic treatment one can now understand the mapping to the one-dimensional lattice already

through the integral, Eq. (3), which is obtained by summing over all terms in the perturbation theory. The fact that all terms contribute "equally" (up to a phase) can be viewed as scattering by a one-dimensional lattice in which every scattering event introduces a phase.

We believe that the connections presented in this work offer many possible venues for extension. Specifically we speculate that through the mapping of Efimov physics to that of a one-dimensional lattice, a possible connection between the Efimov three-body parameter and the geometrical Zak phase [37] for electrons on a one-dimensional lattice could be established. From a mathematical point of view the underlying spiral identified as the underlying fractal structure for the Efimov scattering amplitude might have subtle connections to the Poincaré equation [38].

ACKNOWLEDGMENTS

E.P wishes to thank Gerald Dunne, Eric Akkermans, and Alxander Teplyaev for enlightening discussions on the mathematics of DSI and Vasili Kharchenko and Jia Wang for very valuable discussions on Efimov physics and, especially, thank Luke Rogers for the spiral mapping idea. E.P. acknowledges the kind hospitality of the Physics Department of the University of Connecticut where this work originated.

[1] V. Efimov, Phys. Lett. B **33**, 563 (1970).
[2] V. Efimov, Yad. Fiz. **12**, 1080 (1970) [Sov. J. Nucl. Phys. **12**, 589 (1971)].
[3] P. Naidon and S. Endo, Rep. Prog. Phys. **80**, 056001 (2017).
[4] T. Kraemer, M. Mark, P. Waldburger, J. G. Danzl, C. Chin, B. Engeser, A. D. Lange, K. Pilch, A. Jaakkola, H.-C. Nägerl, and R. Grimm, Nature **440**, 315 (2006).
[5] F. Ferlaino, A. Zenesini, M. Berninger, B. Huang, H.-C. Nägerl, and R. Grimm, Few-Body Syst. **51**, 113 (2011).
[6] B. Huang, L. A. Sidorenkov, R. Grimm, and J. M. Hutson, Phys. Rev. Lett. **112**, 190401 (2014).
[7] S.-K. Tung, K. Jimenez-Garcia, J. Johansen, C. V. Parker, and C. Chin, Phys. Rev. Lett. **113**, 240402 (2014).
[8] R. Pires, J. Ulmanis, S. Häfner, M. Repp, A. Arias, E. D. Kuhnle, and M. Weidemüller, Phys. Rev. Lett. **112**, 250404 (2014).
[9] O. Ovdat, J. Mao, Y. Jiang, E. Y. Andrei, and E. Akkermans, Nat. Commun. **8**, 507 (2017).
[10] P. Zhang and H. Zhai, Front. Phys. **13**, 137204 (2018).
[11] C. Gao, H. Zhai, and Z. Y. Shi, Phys. Rev. Lett. **122**, 230402 (2019).
[12] D. Lee, J. Watkins, D. Frame, G. Given, R. He, N. Li, B.-N. Lu, and A. Sarkar, Phys. Rev. A **100**, 011403(R) (2019).
[13] J. Maji, S. M. Bhattacharjee, F. Seno, and A. Trovato, New J. Phys. **12**, 083057 (2010).
[14] T. Pal, P. Sadhukhan, and S. M. Bhattacharjee, Phys. Rev. Lett. **110**, 028105 (2013); Phys. Rev. E **91**, 042105 (2015).
[15] J. Maji, F. Seno, A. Trovato, and S. M. Bhattacharjee, J. Stat. Mech. (2017) 073203.
[16] R. D. Amado and J. V. Noble, Phys. Lett. B **35**, 25 (1971).
[17] R. D. Amado and J. V. Noble, Phys. Rev. D **5**, 1992 (1972).
[18] P. F. Bedaque, H.-W. Hammer, and U. van Kolck, Phys. Rev. C **58**, R641 (1998).
[19] P. F. Bedaque, H.-W. Hammer, and U. van Kolck, Phys. Rev. Lett. **82**, 463 (1999).
[20] P. F. Bedaque, H.-W. Hammer, and U. van Kolck, Nucl. Phys. A **646**, 444 (1999).
[21] E. Braaten and H. W. Hammer, Phys. Rep. **428**, 259 (2006); Ann. Phys. (N.Y.) **322**, 120 (2007).
[22] Y. Castin, C. Mora, and L. Pricoupenko, Phys. Rev. Lett. **105**, 223201 (2010).
[23] B. Bazak and D. S. Petrov, Phys. Rev. Lett. **118**, 083002 (2017).
[24] D. K. Brattan, O. Ovdat, and E. Akkermans, Phys. Rev. D **97**, 061701(R) (2018).
[25] S. Albeverio, R. Høegh-Krohn, and T. T. Wu, Phys. Lett. A **83**, 105 (1981).
[26] K. Wilson, Phys. Rev. D **3**, 1818 (1971).
[27] G. V. Skorniakov and K. A. Ter-Martirosian, Sov. Phys. JETP **4**, 648 (1957).
[28] E. Akkermans, *Contemporary Mathematics*, Vol. 601 (Am. Math. Soc., Providence, RI, 2013), pp. 1–21.
[29] D. Sornette, Phys. Rep. **297**, 239 (1998).
[30] S. Gluzman and D. Sornette, Phys. Rev. E **65**, 036142 (2002).
[31] K. Weierstrass, *Über continuirliche Functionen eines reelles Arguments, die für keinen Werth des letzteren einen Bestimmten Differentialquotienten besitzen, Königl. Akademie der Wissenschaften, Berlin, July 18, 1872*, reprinted in K. Weierstrass, *Mathematische Werke II* (Johnson, New York, 1967), pp. 71–74.
[32] M. V. Berry and Z. V. Lewis, Proc. R. Soc. A **370**, 459 (1980).
[33] E. Nielsen and J. H. Macek, Phys. Rev. Lett. **83**, 1566 (1999).
[34] A. V. Shytov, M. I. Katsnelson, and L. S. Levitov, Phys. Rev. Lett. **99**, 246802 (2007).
[35] M. Kunitski, S. Zeller, and J. Voigtsberger *et al.*, Science **348**, 551 (2015).
[36] H. Wang, H. Liu, Y. Li *et al.*, Sci. Adv. **4**, eaau5096 (2018).
[37] J. Zak, Phys. Rev. Lett. **62**, 2747 (1989).
[38] G. Derfel, P. Grabner, and F. Vogl, J. Phys. A: Math. Theor. **45**, 463001 (2012).